Separation Science and Technology
Publication details, including instructions for authors and subscription information:
http://www.informaworld.com/smpp/title~content=t713708471

Ultrafiltration of Humic Acid Solution: Effects of Self-dispersible Carbon Black and Cations

J. Lohwacharin[a]; S. Takizawa[a]; S. Ohgaki[a]
[a] Department of Urban Engineering, The University of Tokyo, Tokyo, Japan

To cite this Article Lohwacharin, J. , Takizawa, S. and Ohgaki, S.(2008) 'Ultrafiltration of Humic Acid Solution: Effects of Self-dispersible Carbon Black and Cations', Separation Science and Technology, 43: 7, 1852 — 1870
To link to this Article: DOI: 10.1080/01496390801973722
URL: http://dx.doi.org/10.1080/01496390801973722

Separation Science and Technology, 43: 1852–1870, 2008

ISSN 0149-6395 print/1520-5754 online
DOI: 10.1080/01496390801973722

Ultrafiltration of Humic Acid Solution: Effects of Self-dispersible Carbon Black and Cations

J. Lohwacharin, S. Takizawa, and S. Ohgaki

Department of Urban Engineering, The University of Tokyo, Tokyo, Japan

Abstract: Effects of carbon black (CB) addition on membrane fouling and rejection of macromolecular humic acids (HA) were evaluated by a stirred-cell ultrafiltration unit. Stable CB dispersions increased filtration resistances, but enhanced HA rejection by the membranes. Monovalent and divalent ions affected the filtration resistance of CB solution differently; namely, NaCl solution showed a very high resistance due to the concentration of CB in the diffusion boundary layer near the membrane surface, whereas $CaCl_2$ and $MgCl_2$ solutions showed only cake resistance. The cake layer containing both CB and HA was more easily removed from the membranes than HA-cake layer.

Keywords: Carbon black, humic acids, ultrafiltration, aggregation, fouling

INTRODUCTION

A hybrid adsorption-membrane filtration process is effective in removal of both particulate and dissolved contaminants. The conventional adsorbents such as powdered activated carbon (PAC) are not very effective in the removal of macromolecular humic acids (HA) due to their large molecular sizes and limitations of adsorbent materials i.e. dispersion stability, slow adsorption kinetics, and desorption of HA. PAC was ineffective in removing HA fractions with

Received 4 July 2007, Accepted 28 November 2007
Address correspondence to J. Lohwacharin, Department of Urban Engineering, The University of Tokyo, 7-3-1 Hongo, Bunkyo-ku, Tokyo 113-8656, Japan. Tel.: +81-3-5841-6255; Fax: +81-3-5841-8532; E-mail: jenyuk@env.t.u-tokyo.ac.jp

molecular weight less than 300 or greater than 17,000 daltons (1). PAC cake formation caused a significant flux decline in PAC-filtration systems (1, 2). Hence, new adsorbent materials with high adsorption capacity and lower membrane fouling potentials are being explored.

Carbon black (CB) consists of spheroidal particles with a pronounced ordering of the graphene layers. CB has chemisorbed oxygen complexes, i.e. carboxylic, quinonic, lactonic, or phenolic groups on their surfaces to varied degrees depending on the condition of manufacturing (3). The presence of surface functional groups is beneficial in enhancement of dispersibility and dispersion stability in aqueous solution. Since CB has a large easily accessible surface area for adsorption of macromolecules, CB coupled with UF may possibly shorten the contact time for the removal of HA and emerging macropollutants in a hybrid adsorption-membrane filtration process. However, CB deposition on membrane may cause membrane fouling and increase of filtration resistance.

In this study, the effect of CB particles on fouling characteristics and rejection of HA in ultrafiltration under various filtering conditions was evaluated with a dead-end filtration mode. Hydrophilic CB was used so that it can be easily dispersed in water. With an attempt to explain the effects of ionic strength on flux decline, the factors that affect the colloidal stability and aggregation of CB in water were assessed in coagulation experiments. Improved HA rejection by a hybrid CB-UF process was also investigated at varied ionic strength using different cation species.

MATERIALS AND EXPERIMENTAL SECTION

Carbon Black and Humic Acids

The self-dispersible CB (Aquablack-001, Tokai Carbon, Tokyo, Japan) and coal-based humic acids (HA; Wako Pure Chemical Industries, Ltd. Co., Japan) were used in this study. The CB sol was concentrated in a 20% w/w aqueous solution and stored in a polyethylene (PE) container before being conveyed to the laboratory. The CB is chemically modified by the manufacturer to increase carboxyl groups on the surface so that it can be easily dispersed in water. Particle size distribution in the range of 0.8 nm to 6.54 μm was measured by Nanotrac Particle Analyzer (Nikkiso, Japan) at the wavelength of 780 nm using Dynamic Light Scattering (DLS) measurements. The output signal is mathematically analyzed by Microtrac® Windows software to provide particle size distribution. To obtain a reliable analysis, 400 mg/l mono-disperse silica solution was used as a standard before and after measuring the samples. The size distribution of the CB is illustrated in Fig. 1. The volumetric median size of CB was determined as 130 nm. Surface functional groups were investigated by Fourier transform infrared (FT-IR) spectroscopy (Jasco FT-IR-610, Japan) with JASCO DR-81 Diffuse

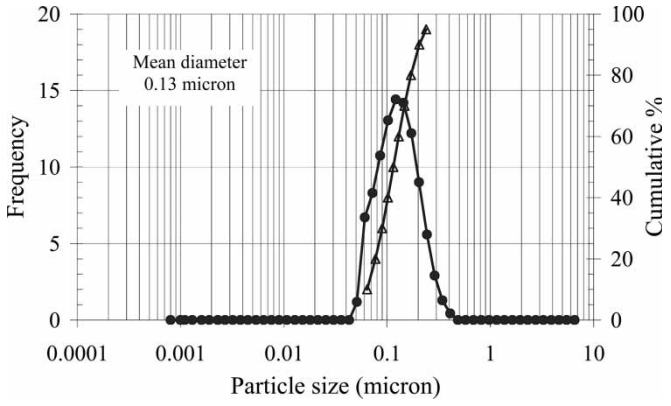

Figure 1. Distribution of CB particle size by DLS measurement. ● A frequency distribution of CB particle size; Δ Cumulative size distribution by particle volume. Note: *Mean diameter* was calculated based on the volume distribution representing the center of gravity of the distribution (obtained by Microtrac™ program).

reflectance attachment at a spectral resolution of 4 cm^{-1} after drying at 105°C for 1 h or lyophilization. The surface charge of CB was measured by acid/base titration (4) with the background NaCl concentration of 1 mM. The pH of CB solution was varied by adding known amounts of 0.025 N NaOH or 0.025 N HCl, then the solution pH was measured to determine the surface charge of CB. The pH at point of zero charge (pH_{pzc}) was defined from the titration curve.

The HA powder was dissolved in Milli-Q water at pH 12 adjusted with 0.1 N NaOH, and then neutralized to pH 7 by 0.1 N HCl. The HA solution thus obtained was filtered with glass fiber filters (nominal pore size 0.30 μm, Advantec GF-75). Characteristics of the HA are given in Table 1. The UV absorbance measured at 280 nm indicated π-π^* electron transitions for a number of aromatic substances and at 465 and 665 nm to determine E_4/

Table 1. Wako HA characteristics (5 mg/L, pH 7 and ionic strength 1 mM)

	UV/Visible absorbance using 10-mm cell			
Wavelength (nm)	254	280	465	665
Absorbance (cm^{-1})	0.114	0.101	0.022	0.005

Note: Spectrophotometric measurements were conducted on a UV/VIS spectrophotometer (HITACHI U-2010). Samples were placed in a 10-mm quartz window cuvette and scanned from 900 to 190 nm. Stock solution was diluted with Milli-Q water and adjusted to pH 7 with 0.1 N HCl. The final ionic strength of 1 mM was adjusted by adding small amount of 0.1 N NaCl.

E_6 ratios, an indicator of humification. The E_4/E_6 ratios of Wako HA was 4.4, which is lower than the reported values of 7.59 and 20.7 for Aldrich HA and Suwannee river fulvic acid, respectively (5).

Membranes and Filtration Procedure

Membrane filtration experiments were performed in a batch stirred cell (Amicon 8050, Millipore) with a capacity of 50 mL, and a geometric membrane area of 13.4 cm^2. Polyethersulfone (PES; Biomax™ PB) membranes with a molecular weight cut-off of 100,000 Da were used in most of the experiments. The flux decline of the PES membrane was also compared with a regenerated cellulose membrane (RC; Ultracel™ PL). Before being used, the preservative and anti-drying agents were removed following the procedure provided by the manufacturers. Dead-end UF was operated at a constant transmembrane pressure (TMP), which was monitored by a digital pressure gauge. Filtrate flux was calculated from the increase of collected permeate measured by a top-loading balance at specified time interval. Standardized flux (J_s) was obtained by correcting all flux values to the standard temperature (25°C) and pressure (1 bar) (6). Hydraulic resistances (R) were calculated by the following equation:

$$J = \frac{\Delta P}{\mu(R_m + R_s + R_p)} \tag{1}$$

where R_m is the hydraulic resistance of the membrane, R_s is the solute resistance, and R_p is the resistance due to pore blockage. The solute resistance consists of cake resistance (R_c) and resistance in the diffusion boundary layer (R_{bl}):

$$R_s = R_c + R_{bl} \tag{2}$$

Flux Decline and Hydraulic Resistances

Solutions containing HA and/or CB were filtered through the PES and RC membranes. The initial concentration of CB and HA solutions were 20 mg/L and 3 mg-C/L, respectively. Solution pH was adjusted to 6.5 (pH_{pzc} of CB) with either 0.1 N HCl or NaOH. The solution was filtered at a constant TMP of 100 kPa and a stirring rate of 600 rpm. After filtration, the fouled membrane was cleaned with pure water to remove the cake layer and the pure water flux using Milli-Q water was obtained to compare the hydraulic resistances after removal of the cake layer. The observed rejections of CB and HA were determined by the following equation using UV/Vis absorbance at 400 and 254 nm, respectively.

$$R(\%) = 100\lfloor 1 - (C_p/C_b)\rfloor \tag{3}$$

where C_p and C_b are CB or HA concentrations in the permeate and bulk fluid in feed solutions, respectively.

To study impacts of CB aggregation on filtration resistances, the filtration resistances of CB cake formed by 3 mM NaCl, 1 mM $CaCl_2$, and 1 mM $MgCl_2$ solutions at pH 7 were evaluated in a single batch using the PES membranes. These solutions thus had the same ionic strength. The salt concentration of 0.2 g/L CB solution was adjusted with the aforementioned salts; and the CB suspension was ultrafiltered at a TMP of 100 kPa and a stirring rate of 600 rpm. At the end of filtration, the bulk CB solution was removed and the cell was carefully filled with Milli-Q water. The cell was gently manually stirred to remove the remained dispersed phase before measuring the cake resistance at 100 kPa without suspended CB in solution. The cake layers formed in these experiments were intact even after replacing the CB solution with Milli-Q water. Since the mean size of CB particles is larger than the membrane pore, the pore blockage resistance (R_p) in Equation (1) can be omitted in this experiment. As a result, boundary layer resistance (R_{bl}) and cake resistance (R_c), could be evaluated by Equations (1) and (2).

Effects of Solution Physico-chemical Properties on a Particle Size of CB

To examine effect of Ca^{2+} and Mg^{2+} concentrations on the particle size distribution of CB, pre-determined volumes of $CaCl_2$ and $MgCl_2$ solutions were added to each 50-mL flask containing 4 mL of 1 g/L CB, and solution pH was adjusted with either 0.1 N NaOH or HCl, before being filled up to a volume of 20 mL by Milli-Q water. Changes of particle size were examined after 10-min, 5- and 72-hour mixing by Nanotrac particle-size analyzer. The effect of NaCl concentration on the size of CB was also investigated using the same ionic strengths as those of $CaCl_2$ and $MgCl_2$ solutions.

RESULTS AND DISCUSSION

Surface Functional Groups and Charge Density

FT-IR spectra of the oven-dried and lyophilized CBs are presented in Fig. 2. In general, sharp peaks can be obtained in the freeze-dried sample because removal of surface-bound water by heat treatment would destroy some heat-sensitive functional groups on the carbon surface. The CB surface was modified by the manufacturer to increase the carboxyl group content. Absorbance at 1720 cm^{-1}, assigned to C═O stretching of carboxyl and carbonyl groups, appears in all samples. We can also find other major features of the CB particles, including -OH at 3750 cm^{-1}, C-H bending at 1457 cm^{-1} in the freeze-dried sample, aromatic C bond at 1508 cm^{-1}, C-O stretching of

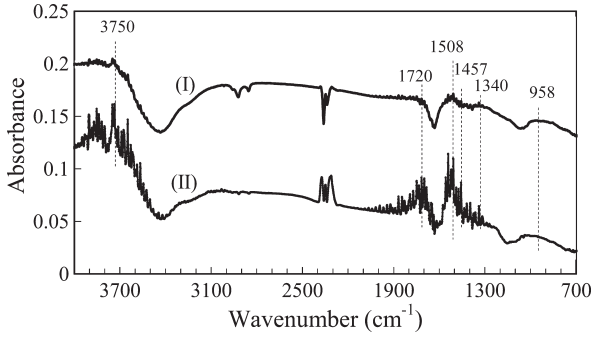

Figure 2. Typical spectra of Aquablack-001 CB at resolution of 4 cm^{-1}. (I) CB sample oven-dried at 105ºC; (II) Lyophilized CB sample.

COOH containing groups with a broad peak at 1340 cm^{-1}, and C-H out of plane at 958 cm^{-1}.

The surface charge density of the CB was measured by acid/base titration. The pH_{pzc} of the carbon was approximately 6.5. It was reported that the pH_{pzc} of activated carbon black composites ranged between 2 and 10.5 (7). Both acidic and basic functional groups exist on the surface of CB. Depending on the treatment of carbons, the acidic character of the surface increases and suppresses the density of basic sites (8). The surface charge of carbon is determined by the numbers and ratio of acidic and basic functional groups. Hence, the overall pH_{pzc} is determined by the numbers of acidic and basic groups.

Ultrafiltration of CB and HA-containing Solutions

Figure 3 shows that dead-end filtration of the HA solution through RC and PES membranes resulted in flux reduction by 8% and 29% after 10-min operation while the flux reduction by 38% and 64% was observed during filtration of CB-HA solution with RC and PES membranes, respectively. These results suggested that the PES membrane, which had a higher initial flux of 1337 Lm^{-2} h^{-1} (lmh) as shown in Table 2 than the RC membrane (726 lmh), suffered from solute resistance due to HA and CB particles more seriously than the RC membrane. With the PES membrane, after the initial decline, normalized flux decreased rapidly on filtration of the HA solution. Inversely, after the initial decay, reduction of normalized flux was more rapid on filtration of CB/HA solution than that of HA solution with RC membranes. The different behavior for the PES and RC membranes might be due to a combination of membrane permeability, hydrophobicity, and surface charge effects.

The extent of initial flux decline was in the order of CB + HA > CB > HA in both membranes (Fig. 3). The RC and PES membranes are considered

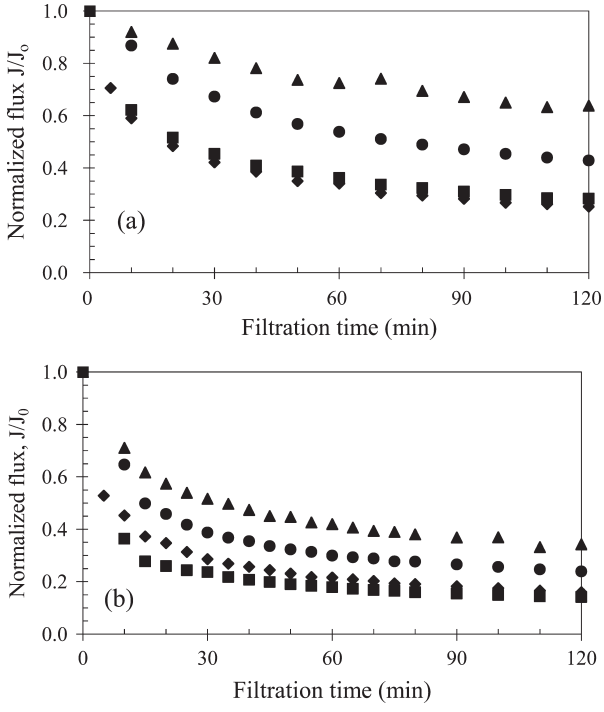

Figure 3. Flux decline of humic acids (HA) and carbon black (CB) solutions. (TMP 100 kPa), (a) Regenerated cellulose (RC) membrane (MWCO 100 kDa); (b) Polyethersulfone (PES) membrane (MWCO 100 kDa); (▲) Humic acid (HA) 3 mg/L in Milli-Q water; (●) Carbon black (CB) 20 mg/L in Milli-Q water; (■) HA (3 mg/L) + CB (20 mg/L) in Milli-Q water; (◆) HA (3 mg/L) + CB (20 mg/L) in 0.5 mM $CaCl_2$ Note: J denotes flux at time t; J_0 denotes clean water flux of virgin membrane under different feed solutions.

to be negatively charged in the experimental condition. The apparent zeta potential for the PES membrane was -15.17 ± 0.8 mV at pH 7 in 10 mM KCl (9) while the composite RC membrane had a zeta potential of -2.2 ± 0.5 mV in similar conditions (10). The large negative charge on the PES membrane induced a significant electrostatic exclusion of negatively charged HA and CB from membrane surface. Both membranes had MWCO of 100 kD and separated the CB particles successfully without a trace of CB in the permeate because the mean size of CB, i.e. 130 nm, was nearly 10 times larger than the membrane-pore size of 14.3 nm, calculated by the following equation (6)

$$d = 0.09(\text{MWCO})^{0.44} \tag{4}$$

where d is in nanometers and MWCO is in daltons. Rejected CB and/or HA molecules formed concentrated solutes in a boundary layer and accordingly

Table 2. Virgin membrane flux (J_0) in lmh ($Lm^{-2}h^{-1}$), total membrane resistance (R), and flux recovery of the membranes (J/J_0) after removal of cake layer by hydraulic cleaning with pure water

	Humic acid			Humic acid & Carbon black			Humic acid & Carbon black 0.5 mM, Ca		
Membr.	J_0 (lmh)[a]	R^b_{HA} ($10^{11}m^{-1}$)	J/J_0	J_0 (lmh)[a]	R^b_{HACB} ($10^{11}m^{-1}$)	J/J_0	J_0 (lmh)[a]	R^b_{HACB} ($10^{11}m^{-1}$)	J/J_0
RC	726	8.28	0.707	717	6.90	0.817	750	5.60	0.939
PES	1337	6.50	0.457	1418	3.57	0.778	1139	17.09	0.208

RC: regenerated cellulose membrane (Ultracel™ PL, Amicon, MWCO 100,000 dalton).

PES: polyethersulfone membrane (Biomax™ PL, Amicon, MWCO 100,000 dalton).

[a] J_0 ($Lm^{-2}h^{-1}$): pure water flux of a virgin membrane with Milli-Q water.

[b] $R = \Delta P/\mu\, J$ where ΔP denotes transmembrane pressure, μ the absolute viscosity (Pa-sec), and J pure water volumetric flux after clean with Milli-Q water.

resulted in substantial hydrodynamic resistance. The relatively large negative charge and high permeability of PES membrane apparently resulted in substantial flux reduction.

The solute can be coagulated in the diffusion boundary layer as the solute concentration reaches a critical value. Back-diffusion of the particles to the bulk solution was controlled by stirring in this experiment. A solute aggregation caused deposition of cake/gel layer with a different degree of affinity to the membrane surface.

As for the hydrophobicity of the membranes, the RC membrane is hydrophilic in nature (11) while the PES membrane, which has a relatively more open microstructure providing fast separation, is hydrophobic with a contact angle of 58 degree (12). Generally a contact angle of over 50 degrees is considered as hydrophobic (13). It was revealed that HA adsorption was greater on the hydrophobic membranes (14). The coal-based HA contained high molecular weight molecules and those molecules might cause flux decay by cake layer formation on the surfaces of both types of membranes, but more strongly adsorb on PES membrane. The continued gradual flux decline might be cake formation by CB and HA, combined with pore blockage by HA.

To study the impact of CB-HA coagulation on flux decline, 0.5 mM $CaCl_2$ was added into a CB-HA solution after CB (20 mg/L) and HA was mixed in a solid-contact chamber for 20 min. 0.5 mM $CaCl_2$ corresponds to the Ca^{2+}/gCB ratio of 25 mmol/g, which was estimated to be effective in aggregation of CB colloids, based on the result shown in Fig. 9 (coagulation started at Ca^{2+}/gCB ratio of 5 mmol/g). It was reported that, at high $CaCl_2$ concentration of 40 mM, the filtration resistance of hematite (mean hydrodynamic diameter 100 nm) decreased dramatically after rapid coagulation occurred (15). In this study, however, the presence of 0.5 mM Ca^{2+} ion had no significant effect on flux decline with RC membrane but slightly increased permeate flux of the PES membrane (Figs. 3(a) and (b)). Hence, to find the effect of CB aggregation on ultrafiltration, a more detailed study was carried out and presented later.

According to Table 2, after the removal of the cake layer by hydraulic cleaning, the filtration resistance of the membranes previously filtered with both HA and CB were lower than those filtered without CB, suggesting that in the presence of CB the membrane fouling can be more easily recovered by hydraulic cleaning. The HA fraction contributing to the irreversible fouling might be adsorbed onto CB surface. It was described that UV-absorbing fraction of HA contributed to irreversible pore adsorption and blockage (11). This conformed the result in Fig. 4(b) that CB enhanced rejection of UV_{254} and consequently increased the flux recovery after cleaning. Addition of 0.5 mM Ca^{2+} ion further improved flux recovery after hydraulic cleaning with J/J_0 increasing to 0.939 with RC membrane. In contrast, the presence of Ca^{2+} ion substantially reduced the flux recovery of CB-HA cake with PES membrane. In UF filtration, the flux decline may be caused by sequential or simultaneous process of surface coverage during filtration (13). Studies in the

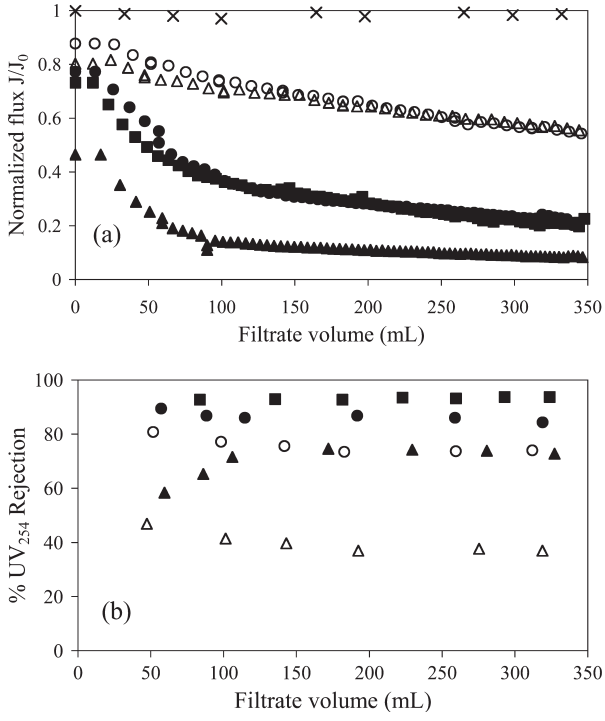

Figure 4. Effects of ionic strength on filtration of HA and CB-HA containing solutions (HA 4 mg/L, CB 40 mg/L, TMP 70 kPa, pH 7, PES membranes). (a) Flux decline as a function of filtrate volume. (×) Pure water flux of a virgin PES membrane, (■) CB-HA in Milli-Q water; (●) 3 mM NaCl CB-HA solution; (▲) 9 mM NaCl CB-HA solution; (○) 3 mM NaCl HA solution (△) 9 mM NaCl HA solution; (b) UV_{254} rejection as a function of filtrate volume. (■) CB-HA solution in Milli-Q water; (●) CB-HA, 3 mM NaCl; (▲) CB-HA, 9 mM NaCl; (○) HA, 3 mM NaCl; (△) HA, 9 mM NaCl. Note: % retention, R was calculate by $R = 100 \times (1 - C_p/C_f)$ where C_f is the concentration in the feed solution and C_p the permeate concentration.

literature have shown fouling in low pressure membrane and its irreversibility to be influenced strongly by the membrane and solution characteristics and presence of macromolecules (16, 17, 12). It was depicted that the flexible macromolecules of HA formed densely packed cake layer (17) while the HA-rigid CB composite cake might be loosely packed with the relatively higher permeability than the HA dense layer.

The effects of ionic strength on flux decline and HA rejections during membrane filtration are presented in Figs. 4(a) and 4(b), respectively. Bulk CB and HA concentrations were 40 mg/L and 4 mg-C/L, respectively. A lower operating pressure (70 kPa) than that in the previous experiment (100 kPa) was used so as to avoid initial deposition and pore blockage by HA molecules. Mild stirring at a rate of 350 rpm was maintained to study

the effect of polarization induced in the presence of NaCl. It was evident that increasing NaCl concentration from 3 mM to 9 mM resulted in flux reduction with the greater extent on filtration of CB-HA solutions. The normalized flux (J/J_0) reduced to 0.54 and 0.55 after passage of 350 mL of filtrates of HA solutions with NaCl concentration of 3 mM and 9 mM, respectively. The CB-HA solutions with the NaCl concentration of 3 and 9 mM caused substantial reduction of the normalized flux (J/J_0) to 0.20 and 0.08, respectively, after 350-mL permeates had been collected. Flux decline on filtration of CB-HA solutions in the absence and presence of 3 mM NaCl was similar in magnitude.

Electrostatic interactions were found to greatly influence the hydraulic resistances of colloidal suspension. The electrostatic repulsion between CB particles decreased as the concentration of NaCl increased. The decrease in flux on increasing NaCl concentration from 3 mM to 9 mM is thereby due to a more close-packed configuration of CB suspension in the boundary layer. The result exhibited in Fig. 5 is evidence to support the effect of concentrated boundary layer on filtration of colloidal suspension in presence of NaCl.

With regard to pore blocking, at high ionic strength, the size of HA molecules becomes smaller allowing for the HA to easily diffuse into the membrane pores and adsorb, with the aid of convective flow (17). Since CB size was relatively larger than the estimated membrane-pore size, the fouling due to pore blockage by CB particles could be excluded. From the morphological viewpoint, the pore constriction was caused by adsorption of small HA molecules and pore blockage resulted from pore plugging of large molecules or colloids. However, in low-pressure membrane (MF/UF), fouling of UF membrane was likely to be caused by cake layer formation (13).

It was reported that fouling during low-pressure MF was more severe at high salt concentration due to the effect of electrostatic shielding causing tighter packing of the charged HA molecules (18). HA molecules tend to be spherical colloids in high ionic strength solutions (19) that might cause more compact cake/gel layer on the surface of membrane and thus substantial hydraulic resistance. The increase of NaCl concentration in this experiment made the HA cake more densely packed and remained even after hydraulic cleansing. On the contrary, the presence of rigid CB particles prevented the CB-HA composite cake from densely packed configuration even in the NaCl solution. Additionally, in the presence of CB, after the cake/gel layer was removed, the recovered flux was the same as that obtained with a virgin membrane. The absolute flux recovery could not be achieved in the membrane filtered with only HA. Even though flux decline was significant when adding CB in the batch filtration, a prolonged operation might be beneficial from complete reversibility of fouling in the presence of CB.

For the rejection of membrane, adsorption of HA molecules onto CB particles enhanced UV_{254} rejection by UF membrane, even in the presence of NaCl. HA retention decreased with increasing solution ionic strength as can be seen from UV_{254} rejection shown in Fig. 4(b). Impact of NaCl on UV_{254} rejection was substantial in the absence of CB particles. The coiled

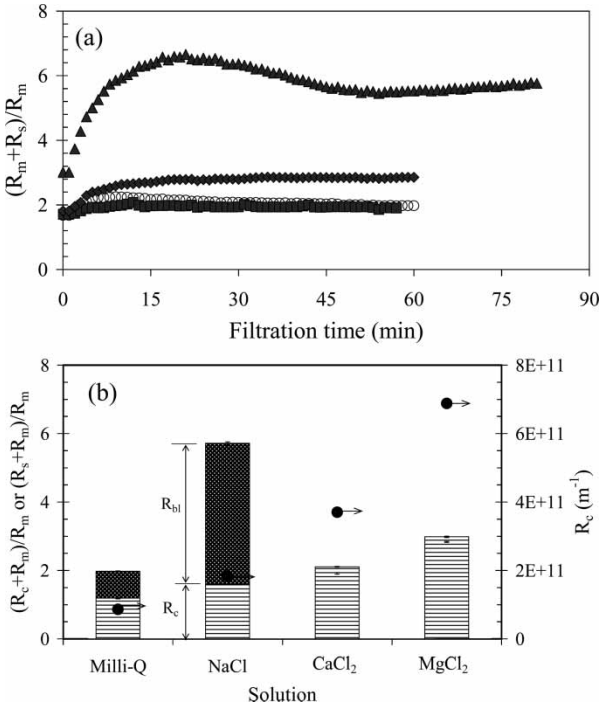

Figure 5. Variation of normalized resistance with filtration time (TMP 100 kPa). (a) (○) CB suspension in Milli-Q water, (▲) CB suspension in 3 mM NaCl, (■) CB suspension in 1 mM $CaCl_2$, (◆) CB suspension in 1 mM $MgCl_2$; (b) Relative contribution of cake resistance R_c to solute resistance R_s ($R_s = R_c + R_{bl}$). (●) Pure water resistance of cake layer (R_c) after removing bulk solution and dispersed CB, (▩) Normalized solute resistance $(R_s + R_m)/R_m$, (▤) Normalized cake resistance $(R_c + R_m)/R_m$, Note: Solute resistance was calculated from $R_s = \Delta P/\mu\, J\ -\ R_m$ where J is filtrate flux at time t and R_m refers the intrinsic hydraulic resistance of virgin membrane. The resistance due to pore blockage (R_p) was excluded due to large size of CB particles. The term "solute resistance" includes resistance (R_{bl}) due to solute concentration in the boundary layer and cake/deposit layer resistance (R_c): $R_s = R_c + R_{bl}$. Cake resistance was obtained after removing bulk CB suspension and filtering with Milli-Q water (TMP 100 kPa). The calculation was carried out as following: $R_c = \Delta\ P/\mu\ J_w\ -\ R_m$ where J_w is pure water flux for cake-fouled membrane at time t and R_m refers the intrinsic hydraulic resistance of virgin membrane. Error bars, referring to the 1SD for an average measurement of last 10 filtrate flux values (final collected volume of 400 mL), are not visible in (NaCl, $CaCl_2$, and $MgCl_2$) because they were smaller than a minor unit of y-axis.

HA molecules in high ionic strength solution might penetrate through micropores of PES membranes whereas stretched HA molecules at low ionic strength would be retained by the size exclusion of the membranes. High salt concentration also had the shielding effect to electrostatic interactions

between negative charges on the membrane surface and negatively charged HA molecules and resulted in the decrease of rejection of low molecular weight HA by the charged membrane.

Ultrafiltration of CB Suspension with Salt Containing Solutions

The effect of CB aggregation, induced by solution chemistry, on filtration resistance during ultrafiltration of CB suspension was demonstrated by adding NaCl, $MgCl_2$, and $CaCl_2$. Solute resistances, including resistance in the boundary layer and cake resistance, were in the order of NaCl $\gg$ $MgCl_2$ $>$ $CaCl_2$ $\sim$ Milli-Q water (Fig. 5(a)). The solute resistance with the NaCl solution was substantial with $R_s + R_m/R_m$ increasing to about 5.72 compared to those obtained in filtration of Milli-Q water or Ca/Mg-containing solutions which had $R_s + R_m/R_m$ as only 1.98, 1.92, and 2.83, respectively. In contrast, the relative resistance due only to cake layer ($R_c + R_m/R_m$) of 1.60 in filtration of NaCl solution was only slightly higher than that obtained with Milli-Q water with $R_c + R_m/R_m$ of 1.19, but significantly lower than those of Ca or Mg-containing waters with $R_c + R_m/R_m$ of 2.11 and 2.98, respectively (Fig. 5(b)). It should be noted that the cake layer in NaCl solution did not cause any significant hydraulic resistance in comparison with the filtration resistance caused by concentrated CB in the diffusion boundary layer near the membrane surface. Electrostatic interactions were found to greatly affect the suspension stability and hydraulic resistance of the cake deposit during ultrafiltration of colloidal particles (20). In our experiments (Figs. 4 and 5), it can be concluded that 3 mM NaCl made CB densely concentrated near the membrane surface than Milli-Q water did, which indicates that an increased ionic strength can shield the electrostatic repulsion of colloidal particles, resulting in more concentrated particles near the membrane surface. These results revealed that the filtration resistance of the NaCl solution was mainly caused by densely concentrated CB near the membrane rather than cake layer formation, whereas cake resistance was dominant in filtration of Ca and Mg-containing solutions.

On the contrary, no suspended CB particle was observed at the end of ultrafiltration of solutions containing Ca or Mg, indicating that all of the coagulated CB was deposited on the membrane. It was reported that during filtration of the unstable colloidal suspension, the increased fluid shear force was no longer able to overcome net attractive forces between the particles and it is therefore not possible to remove accumulated particles in the boundary layer (16). Similarly, in this experiment, stirring was not effective in preventing CB cake formation when rapid aggregation occurred.

Effects of Solution Physico-chemical Properties on CB Aggregation

Since it was found that the addition of NaCl or $CaCl_2$ strongly affected the extent of flux decline on separation of CB particles, the aggregation kinetics of CB

suspension is considered to be an important factor affecting the filtration resistance. Hence, the size distribution of colloidal CB at different mixing time, cationic concentrations, and the pH of 5.8 and 7 was measured by the DLS method. Figure 6 shows the effects of mixing time and cationic concentrations on CB size distribution at pH 7. The size of the CB aggregate increased gradually with mixing time at $CaCl_2$ or $MgCl_2$ concentration of 0.5 mM, but obviously decreased with mixing time at 5 mM after rapid coagulation. The primary particles of CB, which have the smallest size, are typically 13–100 nm in diameter. Aggregates, having the size range of 200–1000 nm, occur in various morphologies, i.e. linear, branched to completely compact, and roughly spherical domain. The largest forms, called agglomerates, have a size exceeding 1000 nm (21). The size of CB at 10 percentile (54–64 nm) measured by DLS at low electrolyte concentrations proves that the CB is composed of primary aggregates which initially tended to interconnect in the presence of divalent cations acting as a bridge to combine negatively charged particles. As the mixing continued, the agglomerates, which consisted of weakly bound aggregates, were broken down into aggregates by the shear

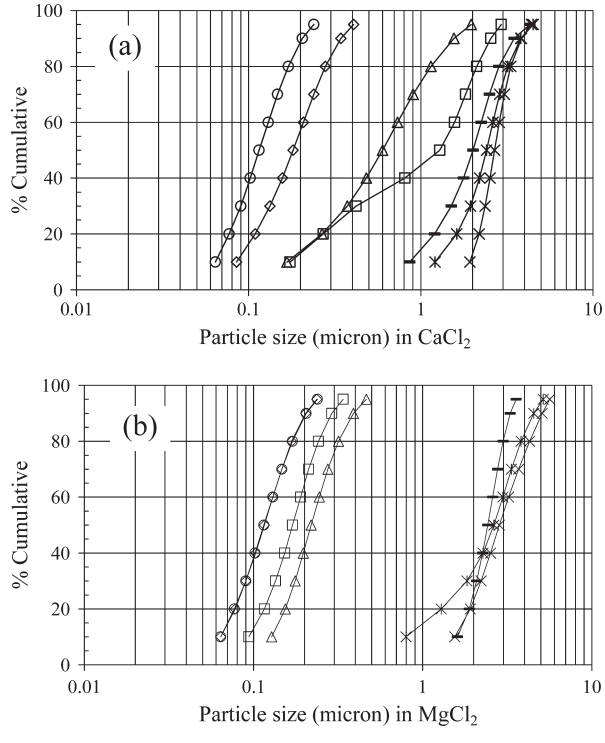

Figure 6. CB size distribution as functions of mixing time and cationic concentrations (CB 200 mg/L, pH7). (a) $CaCl_2$ solution; (b) $MgCl_2$ solution (◇) 0.5 mM, 10 min; (□) 0.5 mM, 5 hrs; (△) 0.5 mM, 72 hrs; (×) 5 mM, 10 min; (✳) 5mM, 5 hrs; (-) 5 mM, 72 hrs; (○) Milli-Q water.

force. Agglomerates formed in the 0.5 mM and 5 mM $CaCl_2$ started to disintegrate after 5-hr and 10-min mixing, respectively when reaching the median size of 1.3 and 2.6 μm, respectively. In 5 mM $MgCl_2$, agglomerates with the median size of 2.8 μm were broken down after 10-min mixing. This result reveals that not only the dose of multivalent ions, but also the mixing time and intensity, are important parameters in controlling cake layer resistance.

The effect of solution pH on the particle size distribution of CB is illustrated in Fig. 7. For both 0.1 mM $CaCl_2$ and $MgCl_2$ solutions, CB sizes at pH 5.8 are presented but overlaid by the data plots at pH 7. At pH 5.8, CB is positively charged due to basic functional groups on the surface of the carbon, whereas CB is negatively charged at pH 7. At the given cationic concentration, the particle size of CB at pH 7 was greater than that at pH 5.8, particularly for 0.5 mM $CaCl_2$ solution. The finding indicated that the aggregation kinetic preferred more negative charges at pH 7 than at pH 5.8. At pH 7, calcium and magnesium ions interacted with deprotonated carboxylic groups while the cations replaced protons in the protonated functional groups to bridge CB particles at pH 5.8. The latter aggregating scenario was confirmed by decrease of solution pH after mixing CB with cationic solution.

In Fig. 8, the effect of different cations at varied concentration is depicted. Experimental result revealed that at ionic strength (I.S.) of 3 mM, NaCl did not

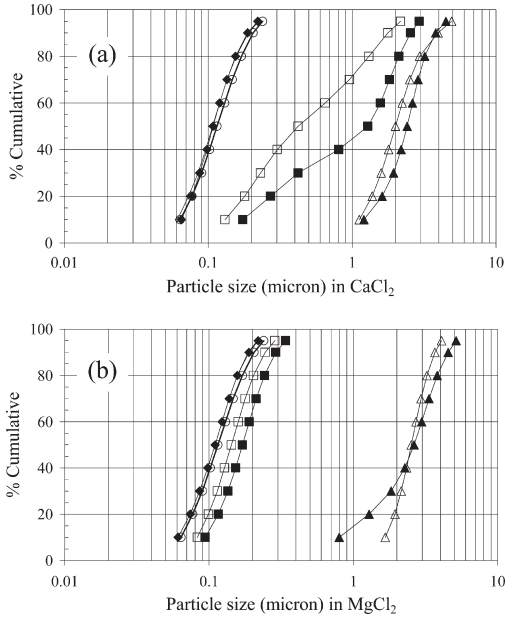

Figure 7. CB size distribution as a function of solution pH (CB 200 mg/L, 5 hrs after mixing). (a) $CaCl_2$ solution, (b) $MgCl_2$ solution (◇) 0.1 mM, pH 5.8 (◆) 0.1 mM, pH 7, (□) 0.5 mM, pH 5.8, (■) 0.5 mM, pH 7, (△) 5 mM, pH 5.8, (▲) 5 mM, pH 7, (○) Milli-Q water.

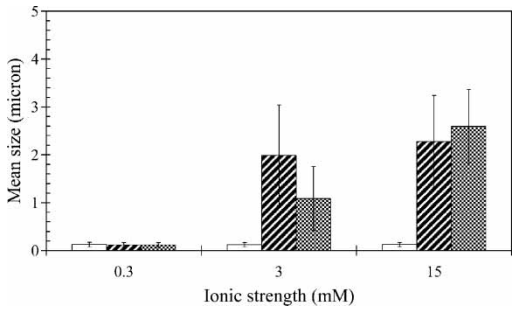

Figure 8. Effects of ionic strength and cations on mean size of CB (CB 200 mg/L, pH 5.8, 5 hrs after mixing). (□) NaCl; (▨) $CaCl_2$; (▩) $MgCl_2$; Note: Error bars indicate SD.

change the particle size distribution of CB; only $CaCl_2$ and $MgCl_2$ caused particle aggregation. At low concentration, $CaCl_2$ was found to be more effective in causing aggregation of CB than $MgCl_2$; namely, the mean diameter of CB at 3 mM was significantly larger for $CaCl_2$ than $MgCl_2$. This difference, however, diminished as the ionic strength increased to 15 mM.

One application of the attained radius (r_{agg}) of the aggregate is to estimate the porosity of the aggregate (ε_{agg}). The porosity of the aggregate can be evaluated according to the relationship (22, 15)

$$\varepsilon_{agg} = 1 - \frac{\rho}{\rho_0} = 1 - \left(\frac{r_{agg}}{a_{prim}}\right)^{D-3} \tag{5}$$

where a_{prim} is the radius of primary particle, ρ the density of an aggregate (total mass of primary particles in the aggregate per encased volume), ρ_0 the density of primary particles, and D is the fractal dimension of the aggregate. It can be seen that fractal dimension and aggregate size have a great effect on the permeability of cake layer and thenceforth the hydraulic resistance of the CB cake layer under a different aggregation regime. The smaller median size of the Mg-CB aggregate compared to that of the Ca-CB aggregate at the cationic concentration of 1 mM, observed previously, suggested that the Mg-CB cake porosity was lower and thus the higher hydraulic resistance.

The results shown in Fig. 9 suggest that divalent cations play a crucial role in aggregation and stability of CB colloids. At Mg^{2+} concentrations of 0.5 mM and lower, the size of CB did not change noticeably. CB particles in $CaCl_2$ solutions were coagulated at the concentration of 0.5 mM. At Ca^{2+} or Mg^{2+} concentrations of 1 mM, the size of CB increases significantly, but further increase of Ca^{2+} concentration to 5 mM did not cause significant increase of CB size. In Fig. 9 the volumetric median size increased drastically from 0.18 μm at 0.5 mM $CaCl_2$ to 2.47 μm at 1 mM $CaCl_2$ after 10-min mixing. The $CaCl_2$ concentration at the middle point of transition was

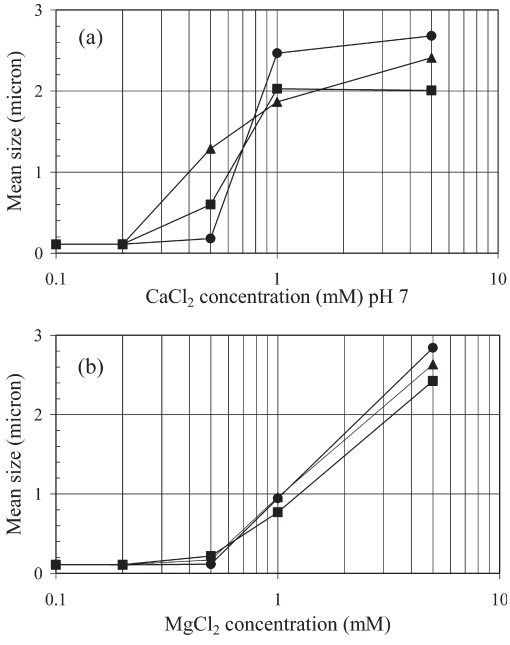

Figure 9. Median size of CB particles as functions of cationic concentration and mixing time (CB 200 mg/L and pH 7). (a) $CaCl_2$ solution, (b) $MgCl_2$ solution; (●) After 10-min mixing; (▼) After 5-hour mixing; (■) After 72-hour mixing.

0.75 mM. The amounts of calcium ions at 0.75 mM corresponded to 7.5 meq/g-CB, which is 19 times higher than the number of acidic functional groups (NaOH uptake) on the CB surface.

CONCLUSION

Carbon black (CB) particles enhanced the rejection of humic acid (HA) by ultrafiltration in the presence and absence of NaCl. The addition of CB particles into the batch filtering process considerably increased filtration resistances but the cake layer formed by CB and HA was more easily removed by hydraulic cleaning than the cake layer made by HA alone. The cake resistance was predominant in the filtration of Ca or Mg-containing solutions, whereas the concentration of dispersed CB near the membrane surface was found to be the major cause of filtration resistance of NaCl solution. The DLS measurement revealed that CB was coagulated in 1 mM Ca or Mg solutions, but remained dispersed in 3 mM NaCl solution. The aggregate characteristics were affected by cationic concentration, mixing time, and solution pH. Hydraulic resistance of CB cake formed under rapid aggregation (with Ca^{2+} or Mg^{2+}) might be related to the cake porosity which increases as the radius of aggregate increases.

SYMBOLS

w/w	Weight by Weight
pH_{pzc}	pH at the point of zero charge
J	Permeate flux ($Lm^{-2}h^{-1}$)
J_0	Pure water flux of a virgin membrane ($Lm^{-2}h^{-1}$)
J_s	Standardized flux ($Lm^{-2}h^{-1}$)
ΔP	Transmembrane pressure (kPa)
μ	Fluid viscosity
R_m	Membrane resistance (m^{-1})
R_s	Solute resistance (m^{-1})
R_c	Cake resistance (m^{-1})
R_p	Resistance due to pore blockage (m^{-1})
R_{bl}	Resistance in the diffusion boundary layer (m^{-1})
UV_{254}	UV absorbance at 254 nm (cm^{-1})
TOC	Total Organic Carbon (mgL^{-1})
r_{agg}	radius of the aggregate (nm)
ε_{agg}	the porosity of the aggregate
a_{prim}	the radius of primary particle (nm)
ρ	the density of an aggregate
ρ_0	the density of primary particles
D	the fractal dimension of the aggregate

ACKNOWLEGDMENT

This study was partially supported by the 21st century COE- Research Project on Sustainable Urban Regeneration provided by the Ministry of Education, Culture, Sports, Science, and Technology (MEXT), of the Japanese Government.

REFERENCES

1. Lin, C.F., Huang, Y.J., and Hao, O.J. (1999) Ultrafiltration processes for removing humic substances: effect of molecular weight fractions and PAC treatment. *Wat. Res.*, 33 (5): 1252.
2. Khan, M.M.T., Kim, H.-S., Katayama, H., Takizawa, S., and Ohgaki, S. (2002) The effect of particulate material and the loading of bacteria on a high dose PAC-MF system. *Wat. Sci. Technol.: Water Supply*, 2 (5–6): 359.
3. Boehm, H.P. (1994) Some aspects of the surface chemistry of carbon blacks and other carbons. *Carbon*, 32 (5): 759.
4. Noh, J.S. and Schwarz, J.A. (1989) Estimation of the point of zero charge of simple oxides by mass titration. *J. Colloid Interface Sci.*, 130 (1): 157.

5. Chin, Y.P., Alken, G., and O'Loughlin, E. (1994) Molecular weight, polydispersity, and spectroscopic properties of aquatic humic substances. *Environ. Sci. Technol.*, 28 (11): 1853.
6. Howe, K.J. and Clark, M.M. (2002) Fouling of microfiltration and ultrafiltration membranes by natural waters. *Environ. Sci. Technol.*, 36 (16): 3571.
7. Trawczyński, J., Suppan, S., Sayag, C., and Djéga-Mariadassou, G. (2002) Surface acidity of the activated CBC. *Fuel Processing Technol.*, 77–78: 317.
8. Ridaoui, H., Jada, A., Vidal, L., and Donnet, J.-B. (2006) Effect of cationic surfactant and block copolymer on carbon black particle surface charge and size. *Coll. Surf. A-Physicochem. Eng. Asp.*, 278: 149.
9. Burns, D.B. and Zydney, A.L. (2000) Buffer effects on the zeta potential of ultrafiltration membranes. *J. Membr. Sci.*, 172: 39.
10. Cheang, B. and Zydney, A.L. (2003) Separation of α-Lactalbumin and β-Lactoglobulin using membrane ultrafiltration. *Biotechnol. Bioeng.*, 83 (2): 201.
11. Aoustin, E., Schäfer, A.I., Fane, A.G., and Waite, T.D. (2001) Ultrafiltration of natural organic matter. *Sep. Purif. Technol.*, 22–23: 63.
12. Lee, N., Amy, G., and Lozier, J. (2005) Understanding natural organic matter fouling in low-pressure membrane filtration. *Desalination*, 178: 85.
13. Lee, N., Amy, G., Croué, J.-P., and Buisson, H. (2004) Identification and understanding of fouling in low-pressure membrane (MF/UF) filtration by natural organic matter (NOM). *Wat. Res.*, 38: 4511.
14. Zeman, L.J. and Zydney, A.L. (1996) *Microfiltration and Ultrafiltration. Principles and Applications*, 1st Edn.; Marcel Dekker: New York.
15. Waite, T.D., Schäfer, A.I., Fane, A.G., and Heuer, A. (1999) Colloidal fouling of ultrafiltration membranes: impact of aggregate structure and size. *J. Colloid Interface Sci.*, 212: 264.
16. Jönsson, A.F. and Jönsson, B. (1996) Colloidal fouling during ultrafiltration. *Sep. Sci. Technol.*, 31 (19): 2611.
17. Jones, K.L. and ÒMelia, C.R. (2001) Ultrafiltration of protein and humic substances: effect of solution chemistry on fouling and flux decline. *J. Membr. Sci.*, 193: 163.
18. Yuan, W. and Zydney, A.L. (1999) Effects of solution environment on humic acid fouling during microfiltration. *Desalination*, 122: 63.
19. Steinberg, C.E.W. (2003) Box 2.1: Structural aspects of the reactivity of humic substances in ecosystems, In *Ecology of Humic Substances in Freshwaters*, 1st Edn.; Springer: Berlin.
20. Bacchin, P., Aimar, P., and Sanchez, V. (1996) Influence of surface interaction on transfer during colloidal ultrafiltration. *J. Membr. Sci.*, 115: 49.
21. Herd, C.R. and Hess, W.M. (1993) In *Carbon Black*, 2nd Edn.; Donnet, J.-B., Bansal, R.C., and Wang, M.J. (eds.); Marcel Dekker: New York.
22. Jiang, Q. and Logan, B.E. (1991) Fractal dimensions of aggregates determined from steady-state size distributions. *Environ. Sci. Technol.*, 25 (12): 2031.